

**Modeling the Impact of Heart Rate Variability on Blood Pressure in
Simulated Atrial Fibrillation Using the BioGears Physiology Engine**

Issac Kim

A thesis

submitted in partial fulfillment of the
requirements for the degree of

Master of Science in Bioengineering

University of Washington

2025

Committee:

Patrick M. Boyle

Austin Baird

Program Authorized to Offer Degree:

Bioengineering

© Copyright 2025

Issac Kim

University of Washington

Abstract

Modeling the Impact of Heart Rate Variability on Blood Pressure in
Simulated Atrial Fibrillation Using the BioGears Physiology Engine

Issac Kim

Chair of the Supervisory Committee:

Patrick M. Boyle

Bioengineering

Atrial fibrillation (AF), the most common sustained cardiac arrhythmia, is characterized by chaotic atrial activation and irregular ventricular response. While its electrophysiologic mechanisms are well studied, the systemic consequences of rhythm irregularity, particularly its impact on blood pressure variability (BPV), remain poorly understood. This study uses the BioGears Physiology Engine, an open-source whole-body simulator, to investigate how RR interval irregularity during AF, quantified by the root mean square of successive differences (RMSSD), influences beat-to-beat hemodynamic stability. Synthetic RR interval sequences were generated to span a physiological AF RMSSD range (80–250 ms) and imposed onto the BioGears cardiovascular model across ten virtual patients. For each simulation, systolic and diastolic BPV were quantified using standard deviation metrics, and linear regression was used to evaluate the relationship between RMSSD and BPV. Results demonstrated a strong positive correlation between RMSSD and both systolic and diastolic BPV across all patients. Simulated BPV values closely matched clinical observations, and a novel phenotype framework was proposed to stratify AF patients by hemodynamic tolerance based on RMSSD-BPV coupling. This work provides a mechanistic link between rhythm irregularity and systemic blood pressure instability in AF and introduces a modeling framework for evaluating arrhythmia tolerance in silico.

ACKNOWLEDGEMENTS

I would first like to express my deepest gratitude to Dr. Patrick M. Boyle, who has been far more than a PI to me. Your mentorship, patience, and constant encouragement have shaped how I think, how I write, and how I carry myself in this field. You believed in me when I didn't have the words or confidence yet, and you gave me the space to figure things out while always holding me to a high standard. This thesis, and my growth as a person during graduate school, would not have been possible without you. I'm grateful beyond words for everything you've taught me; about science, about integrity, and about what it means to be the kind of mentor I hope to be one day. I'm incredibly thankful to have grown under your leadership in the Cardiac Systems Simulation (CardSS) Lab, which has become one of the most meaningful academic communities I've been part of.

To Dr. Austin Baird, thank you for your clear-eyed guidance and technical insight throughout this project. Your ability to help me navigate complexity and see the bigger picture has been invaluable. I've appreciated every meeting, every note, and every reminder to simplify where it matters. To my labmates through the research journey —Savannah, Matt, Chelsea, Jamie, Vicky, and Surbhi—thank you for the laughter, the problem-solving, and the sense of shared momentum. I've learned just as much from our conversations, coding sessions, and shared setbacks as I have from any textbook. To my advisor Whit Fraleigh, and Dr. Wendy Thomas, thank you for being the steady and compassionate presence throughout my studies —always encouraging me to show up authentically. Your belief in me when I didn't believe in myself meant more than I can say. Your advocacy and guidance, especially around diversity and identity in academia, gave me the confidence to take up space and stay true to who I am.

To Dr. Travis Ganje, Mariz, Jes, and Connor, thank you for bringing the clinical lens and for always helping me bridge the gap between my engineering studies and the realities of patient care. You were often the first person I turned to when I felt disconnected from the human side of this work. Your compassion and real-world insight reminded me who this research is ultimately for.

To my family, thank you for raising me to see the world with both logic and heart. Your support has carried me every step of the way. And to RaQuia—thank you for being my home base. Your unwavering belief in me, especially when I struggled to believe in myself, made this possible. This thesis exists because of the generosity, insight, and spirit of everyone named above. I am deeply grateful to have walked this chapter with you.

TABLE OF CONTENTS

List of Figures	ii
List of Tables	iv
Chapter 1. Introduction	1
1.1 Background and Motivation.....	1
1.2 Literature Review & Modeling Context.....	2
1.3 Specific Goals.....	5
Chapter 2. Methodology	6
2.1 Simulation Framework Overview.....	6
2.1.1 BioGears Architecture.....	8
2.2 Patient Model Setup.....	7
2.3 RR Interval Generation and Validation.....	8
2.3.1 RR Interval Modeling Framework.....	8
2.3.2 Generating Target RMSSD Sequences.....	8
2.3.3 RR Interval Statistics and Filtering.....	9
2.4 BPV Extraction and Feature Metrics.....	14
2.5 Model Analysis and Statistical Modeling.....	14
2.5.1 Regression Analysis of RMSSD–BPV Relationship.....	14
2.5.2 Model Evaluation.....	15
Chapter 3. Results	17
3.1 Validation of RMSSD Simulation.....	17
3.2 Blood Pressure Variability Outcomes.....	19
3.3 Regression Modeling of RMSSD–BPV Relationship.....	20
3.3.1 Linear Regression Results.....	20
3.3.2 Sensitivity Across Patient Population.....	23
3.4 Comparison to Clinical Literature.....	31
3.5 Proposed RMSSD-Based Categorization of AF Phenotypes.....	33
Chapter 4. Discussion and Conclusion	36
4.1 Discussion.....	36
4.2 Limitations.....	37
4.3 Future Goals.....	38
4.4 Conclusion.....	39
Reference	40
Appendix	43

LIST OF FIGURES

- Figure 1.1** Conceptual overview of RMSSD and BPV interaction in atrial fibrillation
- Figure 1.2** RR interval patterns in sinus rhythm vs atrial fibrillation. **Top:** Simulated R peaks from a healthy rhythm (black) and atrial fibrillation (red), illustrating increased temporal irregularity in AF. **Bottom:** Corresponding RR intervals over time. AFib exhibits greater beat-to-beat variability and broader deviation from baseline compared to healthy sinus rhythm.
- Figure 1.3.** ECG traces from RR intervals representative of sinus rhythm vs atrial fibrillation. **Top:** ECG trace based on regularly spaced RR intervals representative of sinus rhythm. **Bottom:** ECG trace based on irregularly irregular RR intervals representative of atrial fibrillation.
- Figure 2.1.** Workflow Diagram for RR Interval-Based Simulation of Hemodynamic Variability in AF.
- Figure 2.2.** An overview of the BioGears project architecture, illustrating the Common Data Model (CDM), Synthetic Environment (SE), and the core Physiology Engine.
- Figure 2.3.** Pipeline for RR interval generation and validation.
- Figure 2.4.** Cardiovascular circuit model used in the BioGears Physiology Engine.
- Figure 3.1.** Validation of achieved RMSSD versus target RMSSD, a scatterplot comparing achieved RMSSD versus target RMSSD across all accepted sequences.
- Figure 3.2.** Distribution of simulated AF RR intervals. Histogram of RR interval values from three representative simulations targeting RMSSD values of 80 ms, 150 ms, and 250 ms
- Figure 3.3.** RR Interval Sequences Generated for AF RMSSD = 80 ms and 250 ms. **Top:** R peak timings for low (black) and high (red) AF RMSSD, illustrating differences in temporal regularity. **Bottom:** Corresponding RR intervals plotted over

time. Higher RMSSD sequence (red) exhibits greater beat-to-beat variability compared to the lower RMSSD sequence (black). The dashed blue line indicates the baseline RR interval (800 ms)

Figure 3.3. RR Interval Sequences Generated for AF RMSSD = 80 ms and 250 ms.

Figure 3.4 Time-series trace of simulated systolic and diastolic BP under varying RMSSD

Figure 3.5. Linear Regression of RMSSD vs Blood Pressure Variability. Each point represents a simulation of one virtual patient at a given RMSSD level. Red and blue scatter points show the standard deviation (SD) of systolic and diastolic BP, respectively. Solid lines indicate the linear regression fit with shaded bands showing the 95% confidence intervals.

Figure 3.6 Figure 3.6. Distribution of regression slopes across virtual patients. Bar plot comparing the slope estimates from patient-specific regression models relating RMSSD to BPV .

Figure 3.7 Heatmap of Coefficient of Variation (CV) Across RMSSD Spectrum. Top: Systolic blood pressure coefficient of variation across RMSSD conditions and virtual patients. **Bottom:** Diastolic blood pressure coefficient of variation under the same conditions.

Figure 3.8 Boxplot comparing simulated BPV to clinical literature values.

Figure 3.9 RMSSD-based classification of AF subtypes and their BPV patterns. Each simulation is categorized into: Type I (green): Low RMSSD / Low BPV , Type II (blue): High RMSSD / Low-Moderate BPV , or Type III (red): High RMSSD / High BPV .

Chapter 1. INTRODUCTION

1.1 BACKGROUND AND MOTIVATION

Atrial fibrillation (AF) is the most common sustained cardiac arrhythmia, affecting over 33 million individuals worldwide and contributing substantially to morbidity and mortality through its associations with stroke, heart failure, and systemic embolism [1,2]. Defined by chaotic atrial activation and an irregularly irregular ventricular response, AF disrupts coordinated myocardial contraction and impairs hemodynamic regulation [3]. While the electrophysiological mechanisms underlying AF initiation and maintenance have been extensively studied [4,5], the systemic consequences of short-term heart rate irregularity, particularly its impact on blood pressure variability (BPV), remain poorly characterized. The interaction between rhythm irregularity and systemic hemodynamic response is schematically illustrated in **Figure 1.1**, which outlines the hypothesized causal pathway from RR interval variability measured via root mean square of successive differences (RMSSD) to BPV, and ultimately to clinical outcomes such as cerebral hypoperfusion or organ dysfunction.

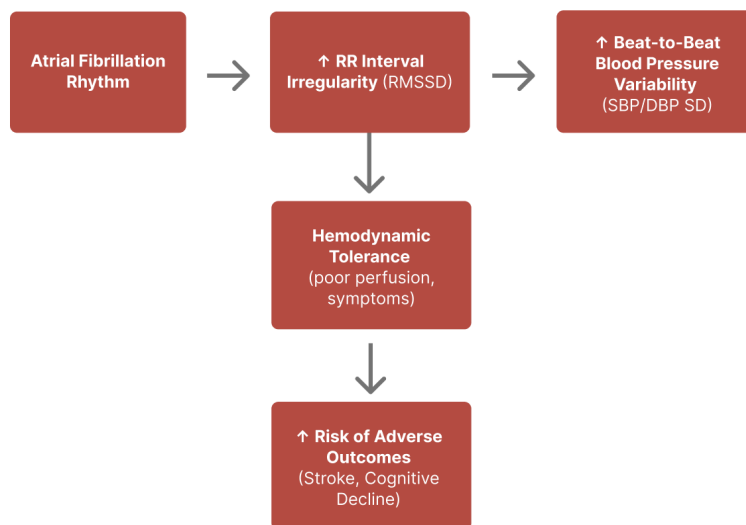


Figure 1.1 Conceptual overview of hypothesized RMSSD and BPV interaction during AF.

RMSSD is a time-domain metric of heart rate variability (HRV) that captures high-frequency fluctuations in RR intervals and is commonly interpreted as a surrogate for parasympathetic tone. In healthy sinus rhythm, RMSSD reflects autonomic modulation and typically ranges between 20–70 ms. In atrial fibrillation, by contrast, disordered atrial activity leads to a highly irregular ventricular response and elevated RMSSD values, often exceeding 100 ms [6]. Representative RR interval patterns in atrial fibrillation and sinus rhythm are shown in **Figure 1.2**. To illustrate how this timing irregularity affects cardiac signals, **Figure 1.3** presents ECG traces generated using sinus-like versus AF-like RMSSD sequences.

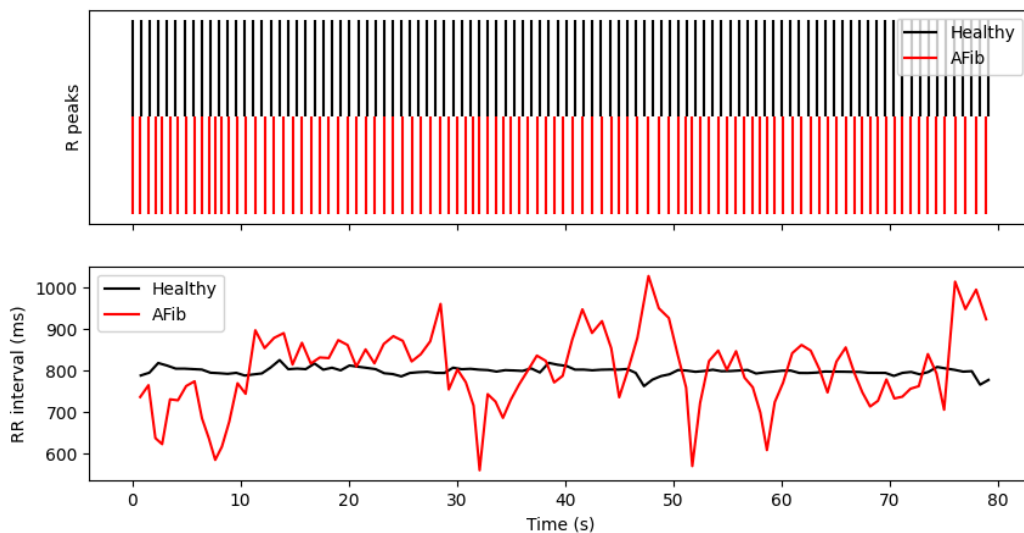


Figure 1.2 RR interval patterns in sinus rhythm vs atrial fibrillation. Top: R peaks from a healthy rhythm (black) and atrial fibrillation (red), illustrating increased temporal irregularity in AF. **Bottom:** Corresponding RR intervals over time. AFib exhibits greater beat-to-beat variability and broader deviation from baseline compared to healthy sinus rhythm.

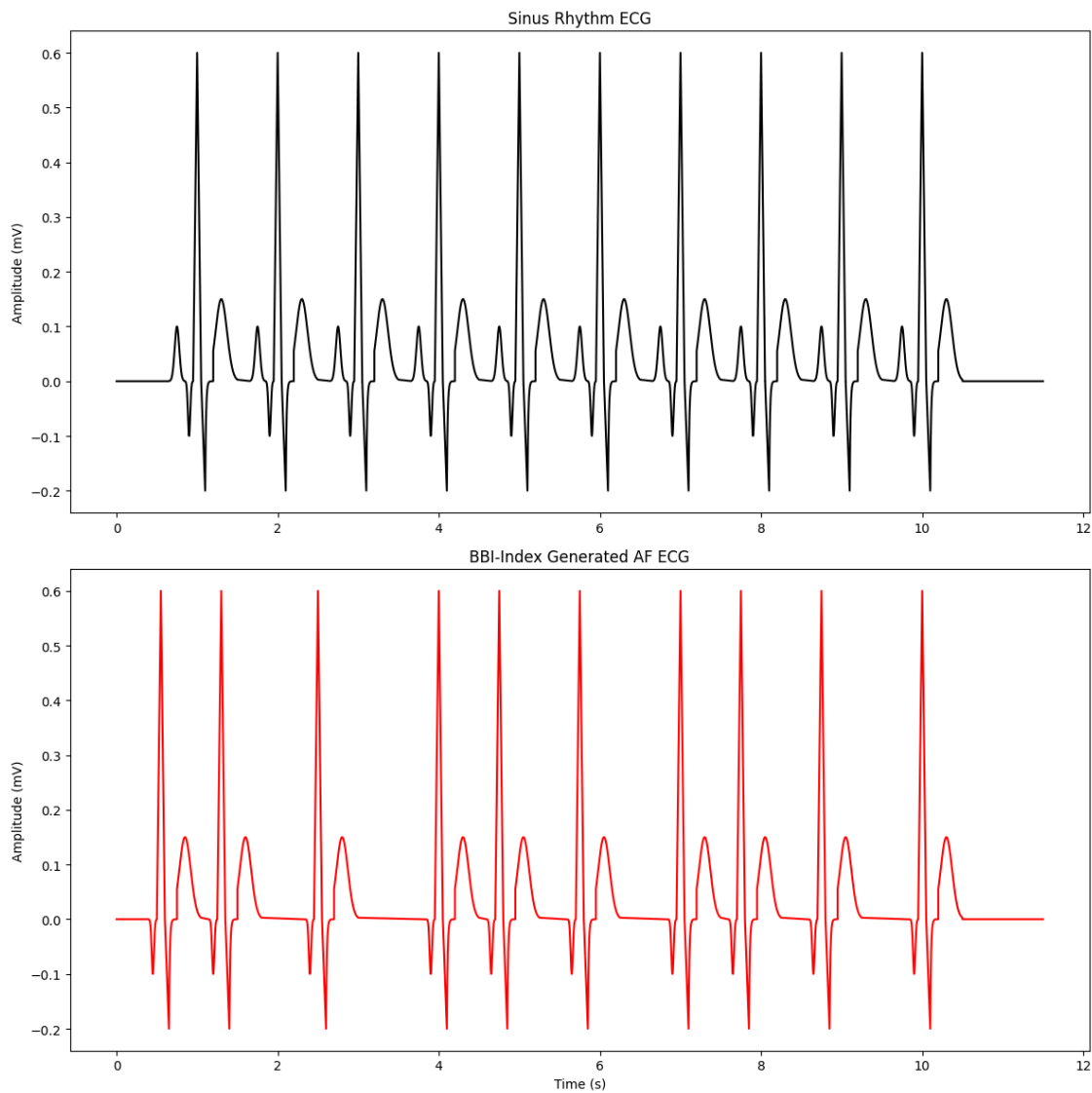


Figure 1.3 ECG traces from RR intervals representative of sinus rhythm vs atrial fibrillation. **Top:** ECG trace based on regularly spaced RR intervals representative of sinus rhythm. **Bottom:** ECG trace based on irregularly irregular RR intervals representative of atrial fibrillation. * Waveform morphology was held constant; only the timing of depolarizations varies between traces for the purposes of this figure.

Although BPV has been recognized as an independent predictor of cardiovascular outcomes, including stroke and end-organ damage [7,8], its relationship with RR interval irregularity during AF has received limited mechanistic exploration. Clinical observations

suggest that greater beat-to-beat RR variability may exacerbate BP fluctuations, compromising cerebral autoregulation and increasing the risk of hypoperfusion-related complications [9].

Simulation-based approaches offer a powerful means to explore causal physiological relationships under controlled conditions. The BioGears Physiology Engine, an open-source, whole-body simulation platform, provides a validated framework for modeling dynamic interactions among cardiovascular, respiratory, and autonomic systems [10]. Its modular architecture supports real-time manipulation of cardiac rhythm, vessel compliance, and regulatory feedback, enabling the exploration of systemic responses to pathophysiological perturbations. BioGears has been applied to model hemorrhagic shock, pharmacokinetics, and ventilatory failure, yet has not been previously leveraged to study the hemodynamic consequences of RR interval irregularity in AF [11].

The absence of established modeling frameworks linking HRV metrics to systemic outcomes in AF presents a critical gap in current simulation literature. Specifically, the influence of varying RMSSD levels on systolic and diastolic BPV remains undefined, despite its potential clinical relevance for stratifying AF subtypes and guiding rate control strategies. Emerging evidence supports the hypothesis that hemodynamic tolerance to AF may differ significantly based on the pattern and degree of RR interval irregularity [18]. In this context, simulation-based evaluation of RMSSD-driven BP fluctuations may aid in identifying arrhythmia phenotypes with distinct cardiovascular risk profiles.

This study addresses the need for an integrative, mechanistic framework to characterize the systemic consequences of RR interval irregularity in AF. By simulating a range of RMSSD conditions within the BioGears engine and quantifying resultant BPV, this work aims to establish a physiologically grounded relationship between atrial rhythm irregularity and systemic

hemodynamic disruption. Such modeling efforts may ultimately support the development of personalized management strategies based on electrophysiological and hemodynamic phenotyping.

1.2 LITERATURE REVIEW & MODELING CONTEXT

AF presents with substantial inter-patient variability in rhythm patterns and hemodynamic tolerance. This variability complicates therapeutic decision-making, particularly in rate control strategies, and poses challenges for predictive modeling. One of the primary metrics used to quantify RR interval variability is the RMSSD, a time-domain measure of HRV that reflects short-term irregularity. In patients with AF, RMSSD is often elevated compared to those in sinus rhythm and has been proposed as a descriptor of irregularity burden rather than autonomic tone [6].

Across AF populations, studies have reported wide-ranging RMSSD values, with means ranging from below 30 ms in paroxysmal AF to over 200 ms in patients with vagal-dominant or structurally mediated arrhythmia [17,18]. For instance, Liu et al. documented significantly different RMSSD profiles in vagally versus sympathetically triggered AF onset, with values of 170.43 ± 94.4 ms and 86.15 ± 45.5 ms, respectively, suggesting that autonomic pathways significantly shape the variability profile [19]. In another cohort involving patients with hypertrophic cardiomyopathy and AF, RMSSD averaged 43.9 ± 27.2 ms, indicating the potential modifying influence of structural heart disease [20]. While such studies provide a quantitative framework for RR variability in AF, few have directly explored the systemic implications of these differences.

BPV, particularly beat-to-beat systolic and diastolic fluctuations, has been independently associated with stroke risk, cognitive impairment, and mortality [7,8]. Although RR interval

irregularity has long been assumed to drive BPV in AF, the relationship has not been systematically dissected. Early studies involving induced AF during electrophysiology procedures revealed that irregular RR intervals alone, when rate was held constant, could destabilize stroke volume and increase BPV, emphasizing that rhythm irregularity is not merely an epiphenomenon but a potential causal factor in hemodynamic compromise [23].

Emerging evidence further suggests that hemodynamic tolerance to AF is not uniform across individuals and may depend on the degree and pattern of RR interval irregularity. Clark et al. demonstrated that greater irregularity was associated with worsened cardiac output and increased pulmonary pressures, independent of rate [24]. Ko et al. found that RR interval scatter significantly influenced beat-to-beat left ventricular performance in AF patients, reinforcing the clinical importance of rhythm irregularity [25]. More recently, Sramko et al. reported that irregularity, in combination with atrial contractile loss, resulted in the most severe hemodynamic impairment during simulated AF episodes [26].

Most computational efforts in AF modeling have centered on atrial electrophysiology or arrhythmia propagation rather than systemic consequences. Cellular and tissue-level models, such as the Courtemanche-Ramirez-Nattel model or openCARP, have been instrumental in studying action potential duration, reentry dynamics, and pharmacologic response [24,25]. However, these frameworks are not designed to evaluate systemic hemodynamics, as they lack integrated feedback systems such as vascular compliance, autonomic control, or organ-level blood flow dynamics.

The BioGears Physiology Engine offers a compelling alternative for bridging this gap. BioGears is an open-source, whole-body simulation platform that models cardiovascular, respiratory, renal, and neurological systems with real-time feedback and pharmacodynamic

capabilities [10]. Its cardiovascular module includes representations of baroreflex sensitivity, venous return, ventricular elastance, and autonomic feedback loops. Previous applications of BioGears have demonstrated its utility in simulating trauma, drug metabolism, and ventilator management, but to date, no published studies have applied the engine to model rhythm irregularity in AF or its impact on BPV.

A mechanistic framework that links RR interval irregularity (e.g., RMSSD) to BPV in AF is needed to quantify this relationship and explore its clinical implications. Modeling this interaction under controlled simulation conditions allows for the isolation of rhythm variability as a single modifiable parameter, facilitating causal inference. Such an approach may enable the future classification of AF subtypes based on rhythm-hemodynamic signatures and inform rate control thresholds tailored to individual tolerance profiles.

1.3 SPECIFIC GOALS

Despite the established clinical relevance of both heart rate variability and blood pressure variability in atrial fibrillation (AF), the direct mechanistic relationship between RR interval irregularity and systemic hemodynamic disruption remains insufficiently defined. Current computational tools used to study AF either lack whole-body integration or are not designed to assess downstream circulatory effects. As such, a physiologically grounded framework capable of isolating the impact of RR interval variability on cardiovascular output is needed to inform AF subtyping, guide therapy, and generate hypotheses for experimental validation.

The objective of this study is to systematically evaluate how varying degrees of RR interval irregularity, quantified using RMSSD, influence beat-to-beat BPV during simulated atrial fibrillation using the BioGears Physiology Engine. By simulating a range of RMSSD profiles across multiple virtual patient configurations, this investigation aims to characterize the causal

effect of rhythm irregularity on systolic and diastolic blood pressure variability, independent of confounding factors such as atrial contraction or pharmacologic input.

The specific goals of this study are:

1. **To implement simulated atrial fibrillation rhythms in BioGears by generating and imposing synthetic RR interval sequences with controlled RMSSD values,** spanning the clinical range observed in AF populations (approximately 80–250 ms).
2. **To evaluate the relationship between RMSSD and short-term BPV,** quantified by the standard deviation of systolic and diastolic blood pressure across steady-state simulation periods.
3. **To assess inter-patient variability in RMSSD–BPV coupling,** using parameter-diverse virtual patient profiles to determine the robustness and generalizability of observed trends.
4. **To compare simulated BPV values with clinical literature,** validating the physiologic plausibility of BioGears outputs and identifying convergence or divergence with empirical data.
5. **To explore the potential for RMSSD-based classification of AF subtypes,** by identifying threshold ranges of RR irregularity associated with distinct hemodynamic profiles.

By achieving these goals, this study seeks to establish a novel computational basis for understanding the systemic consequences of RR interval irregularity in atrial fibrillation and to support the development of rhythm-specific, physiology-informed therapeutic strategies.

Chapter 2. METHODOLOGY

2.1 SIMULATION FRAMEWORK OVERVIEW

All simulations were conducted using the BioGears Physiology Engine (version 7.1), an open-source, human-scale simulation platform designed to represent multiscale physiological interactions across organ systems in real time. The engine integrates cardiovascular, respiratory, neurological, renal, and pharmacokinetic modules within a modular architecture that supports feedback control and perturbation modeling. It has been previously validated for simulating hemorrhagic shock, fluid resuscitation, ventilatory support, and pharmacodynamic interventions under a wide range of physiological conditions[11].

In the present study, BioGears was used to isolate and examine the hemodynamic consequences of RR interval irregularity in the setting of AF. The simulation framework was configured to disable native pacemaker activity and override ventricular pacing through externally supplied RR interval sequences. These sequences were synthetically generated to match predetermined RMSSD targets, thereby allowing direct control over the degree of rhythm irregularity injected into the model. Atrial systole was not simulated, reflecting the absence of coordinated atrial contraction in AF.

Each simulation was initialized under normovolemic baseline conditions with default cardiovascular parameters derived from the BioGears standard male patient profile. The baroreflex feedback loop remained active throughout all simulations to preserve autonomic compensation in response to hemodynamic disturbances. No pharmacological agents were administered, and other pathological states (e.g., sepsis, trauma, or structural heart disease) were excluded to minimize confounding variables.

Simulations were performed in headless batch mode with command-line automation to process multiple RMSSD conditions and virtual patients. For each run, a 60-second stabilization period preceded a 300-second steady-state window, during which output variables were recorded at 1 Hz. Key output signals included aortic systolic and diastolic pressure, mean arterial pressure (MAP), stroke volume, and the full RR interval time series. These outputs were exported in CSV format and analyzed post hoc using R (version 4.3) and Python (version 3.10) for feature extraction and visualization. A schematic overview of the simulation process, including RR interval generation, BioGears configuration, and downstream analysis, is shown in **Figure 2.1**.

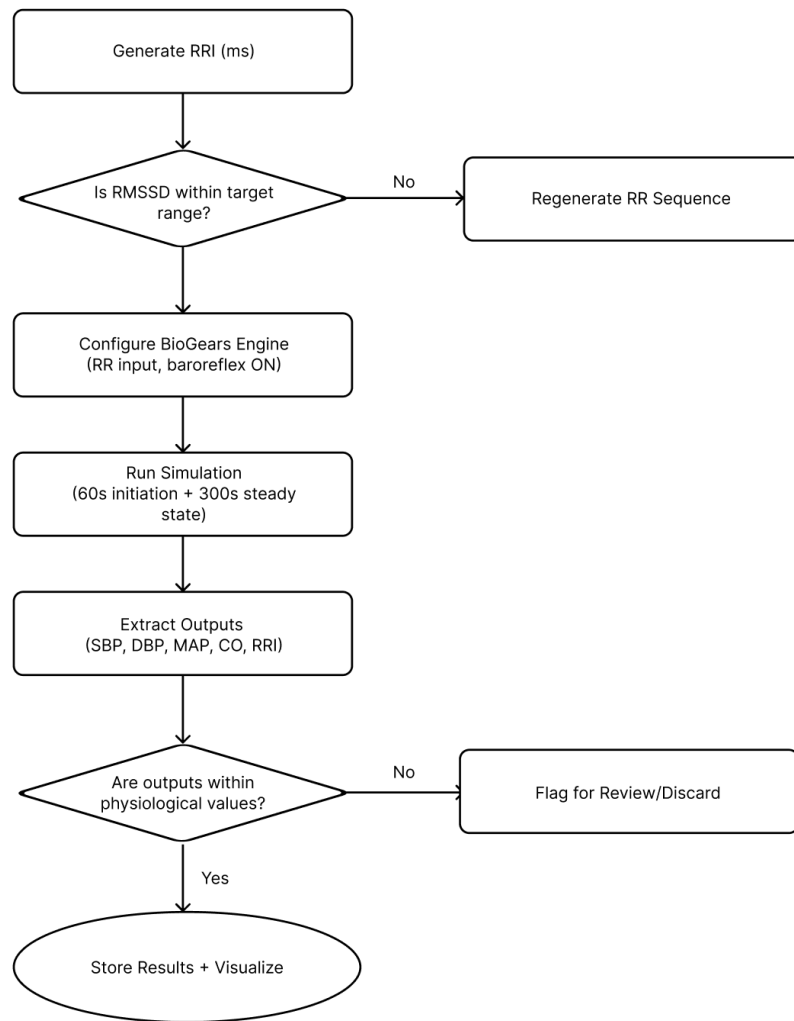


Figure 2.1 Workflow Diagram for RR Interval-Based Simulation of Hemodynamic Variability in AF. RR interval (RRI) sequences are generated to approximate target RMSSD

values. If the achieved RMSSD falls outside a defined tolerance range, the sequence is regenerated. Valid sequences are injected into the BioGears engine for simulation under atrial fibrillation-like conditions. Simulation outputs are extracted and compared to literature values for physiological plausibility prior to final analysis and visualization.

2.1.1 *BioGears Architecture*

The BioGears Physiology Engine is an open-source, C++-based human-scale simulation platform developed by Applied Research Associates [11]. Designed for modeling integrated physiology in real time, BioGears supports simulations of cardiovascular, respiratory, metabolic, and pharmacologic processes within a unified systems framework [11,12]. Its modular design and extensible interface make it suitable for educational, clinical, and research applications [13].

The engine consists of three primary components: the Common Data Model (CDM), the Synthetic Environment (SE), and the BioGears Core Engine.

Common Data Model (CDM)

The CDM defines a standardized schema for physiological data exchange. Simulation states, configurations, and results are represented in XML, with structure defined through Extensible Schema Definitions (XSD). This format enables interoperability between systems, improves transparency, and facilitates automated data handling [14]. Developers can generate native bindings from the schema, allowing integration of simulation components across languages and platforms [11].

Synthetic Environment (SE)

The SE provides an object-oriented application programming interface (API) that abstracts key physiological concepts such as patient states, substances, compartments, and units [11]. This

abstraction layer decouples the simulation logic from implementation details, allowing multiple engines with different numerical solvers or fidelity levels to interoperate under the same schema. The SE also supports unit-safe scalar operations and time-dependent physiological processes [15].

BioGears Engine Core

At its core, BioGears employs lumped-parameter models based on electrical circuit analogs, extending the classic Windkessel model of circulation [12,16]. These analogs simulate organ-level and systemic hemodynamics using resistors and capacitors to represent vascular resistance and compliance. Cardiac pumping is modeled through dynamically modulated compliance curves, calibrated to reproduce physiological pressure-volume loops [17]. The respiratory system, drug transport, and tissue-level gas exchange are implemented using similar lumped representations [13].

BioGears structures simulation spaces into compartments, hierarchically organized to represent vascular, interstitial [11], and intracellular spaces. A central Compartment Manager updates these volumes every cycle based on solver outputs, maintaining mass balance and enabling realistic simulation of gas exchange, drug kinetics, and systemic transport [14].

This architecture supports real-time simulations and direct user control over physiological inputs. In this study, the BioGears engine was leveraged to inject custom-generated RR interval sequences with varying RMSSD values, enabling controlled perturbation of cardiac rhythm and observation of downstream effects on blood pressure regulation.

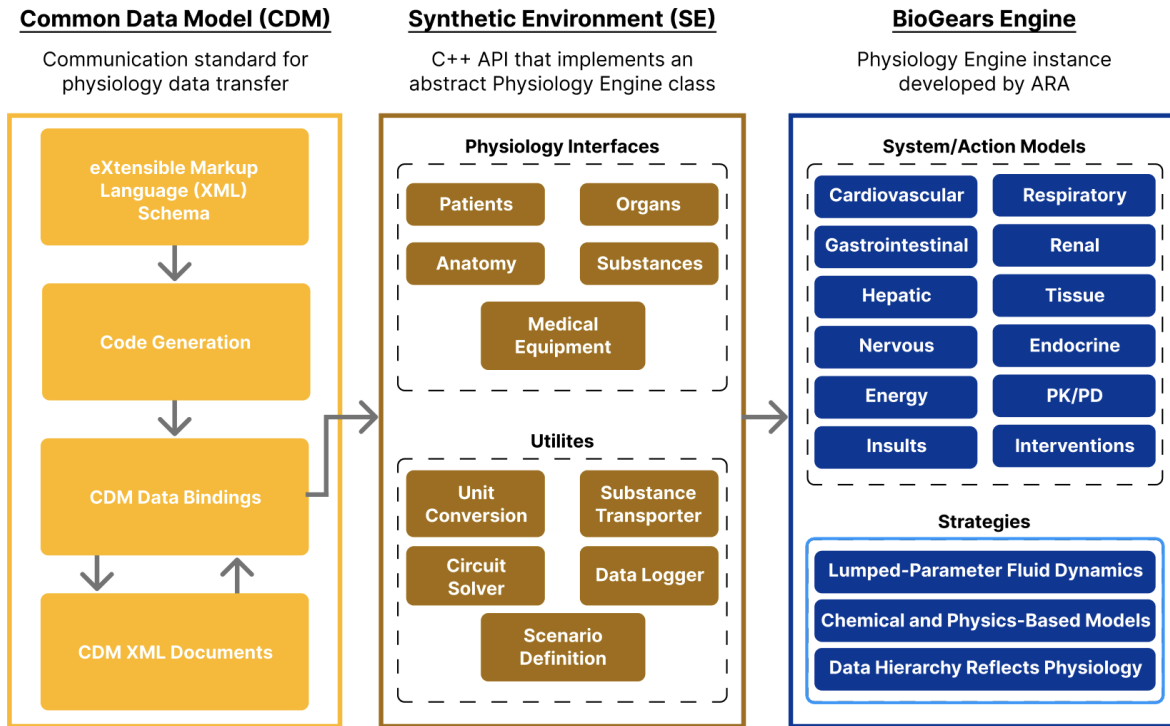


Figure 2.2 An overview of the BioGears project architecture, illustrating the Common Data Model (CDM), Synthetic Environment (SE), and the core Physiology Engine.

2.2 DATA EXTRACTION AND PREPROCESSING

To evaluate the generalizability of RR interval irregularity effects across a range of physiological conditions, simulations were conducted on a set of parameter-diverse virtual patients derived from the default BioGears adult male profile. Each virtual patient was defined by a fixed set of baseline values that remained constant across all RR interval conditions. For example, one patient may exhibit higher vascular compliance and lower resting heart rate, while another may be modeled with reduced compliance and elevated afterload. This approach allows for evaluation of whether the relationship between RR interval variability and blood pressure variability (BPV) is modulated by intrinsic cardiovascular properties.

The full set of simulated patient parameters is summarized in Table 2.1. All patients underwent simulation with each target AF RMSSD value, spanning approximately 80–250 ms.

No structural heart diseases, pharmacologic agents, or pathologic stressors were introduced in order to isolate the interaction between rhythm irregularity and baseline cardiovascular state.

By holding patient-specific parameters constant across all RMSSD levels, intra-patient comparisons of BP variability were enabled, and inter-patient comparisons allowed assessment of systemic tolerance variability. Baroreflex function was preserved across all models, enabling autonomous compensation for irregular preload and pressure fluctuations induced by variable RR intervals.

2.3 RR INTERVAL GENERATION AND VALIDATION

2.3.1 *RR Interval Modeling Framework*

To evaluate the isolated effects of rhythm irregularity on systemic blood pressure, a Beat-to-Beat Irregularity (BBI) model was developed to generate RR interval sequences with controlled levels of short-term variability. This approach allowed the simulation of AF-like rhythm profiles while systematically manipulating the RMSSD as the primary control variable.

RR Interval Generation Components

RR intervals were generated by iteratively computing each new RR interval (RR_{new}) as a weighted combination of a stochastically perturbed prior interval and a baseline target interval. The formulation is:

$$RR_{new} = (1 - \alpha)(RR_{prev} + \delta + \xi) + \alpha \cdot \beta$$

Where:

- RR_{prev} is the previous RR interval
- δ is a perturbation term from a log-normal distribution
- ξ is a short-term variability term sampled from a zero-mean normal distribution with

standard deviation equal to the desired RMSSD

- β is a baseline RR interval drawn from a normal distribution centered at the target RR interval
- α is the “attraction” parameter ($0 \leq \alpha \leq 1$) controlling the cumulative deviation/attraction toward the target

This formulation captures both the long-tailed stochastic behavior and high-frequency variability characteristic of AF, while preserving control over statistical properties.

Parameter Values and Distributions

The generation model used the following parameters and distributional assumptions unless otherwise noted:

- **Target mean RR interval:** 700 ms (0.7 s), corresponding to ~86 bpm.
- **Standard deviation of RR intervals:** 155 ms
 - Based on reported telemetry from clinical AF studies and rhythm databases, RR interval sequences were centered at a target mean of 700 ms (corresponding to ~86 bpm) with a standard deviation of 155 ms. These values fall within the commonly observed ranges for RR interval dynamics in paroxysmal and persistent AF, as described in both clinical literature [21,22] and public AF datasets (e.g., MIT-BIH AFDB)
- **RMSSD:** Varied between 30–250 ms across simulations; 220 ms used for baseline tests
- **Baseline term (β):** Sampled from $\mathcal{N}(\text{RR}_{\text{target}}, \text{SD})$; $\mathcal{N}(0.7, 0.155)$, maintaining realistic clustering
- **Perturbation term (δ):** Drawn from a log-normal distribution, reflecting the right-skewed, heavy-tailed nature of RR intervals in AF; $\mu = \ln(0.7)$, $\sigma = 0.221$

$$\delta \sim \text{LogNormal}(\mu_{\log}, \sigma_{\log}), \mu_{\log} = \log(RR_{\text{target}}), \sigma_{\log} = \frac{SD}{RR_{\text{target}}}$$

- **Short-term variability term (ξ):** Sampled from $\mathcal{N}(0, \sigma = \text{RMSSD})$ to control high-frequency beat-to-beat interval fluctuations
- **Attraction parameter (α):** Values between 0.1 and 0.5 were evaluated; $\alpha = 0.3$ was selected to promote persistent irregularity while maintaining physiologic realism.

These values served as the default configuration for the Beat-to-Beat Irregularity (BBI) model and were held constant across simulations.

2.3.2 *Generating Target RMSSD Sequences*

To simulate varying levels of rhythm irregularity representative of AF, synthetic RR interval (RRI) sequences were generated to match a set of target RMSSD values. RMSSD was selected as the primary measure of short-term heart rate variability. Target RMSSD values were chosen to span a broad physiological range based on reported clinical measurements in AF populations, ranging from 80 ms (minimally irregular) to 250 ms (highly irregular).

RRI sequences were generated using a Gaussian noise-based approach, in which a base heart rate of 75 beats per minute (corresponding to a mean RRI of 800 ms) was modulated with zero-mean white noise. For each target RMSSD, the standard deviation of the noise term was iteratively tuned until the resulting sequence achieved the desired RMSSD value over a 5-minute interval. The final sequences were constrained to remain within physiologically plausible bounds (e.g., 300–2000 ms), avoiding extreme bradycardia or tachycardia.

All intervals were assumed to represent ventricular depolarizations; no ectopy, beat classification, or atrial conduction behavior was modeled. This approach mimicked the irregular but

non-ectopic rhythm seen in AF, with uniform depolarization morphology and no atrioventricular dissociation.

2.3.3 *RR Interval Statistics and Filtering*

Representative RR interval sequences generated for target AF RMSSD values of 80 ms (moderate irregularity) and 250 ms (severe irregularity) to illustrate the contrast between less and more variable rhythms. These sequences, produced by the BBI model, served as direct simulation inputs and highlight the spectrum of temporal dispersion characteristic of different AF profiles. Each generated RRI sequence underwent validation before use in simulation. For each sequence, the achieved RMSSD was calculated and compared to the target. Sequences that fell outside a ± 5 ms tolerance were regenerated by adjusting the noise standard deviation until acceptable accuracy was achieved.

Second, sequences were visually inspected to confirm that the RRI pattern resembled physiologic AF, marked by irregularity without periodicity or long pauses. This inspection was purely qualitative and served as a preliminary sanity check to confirm that the generated sequences visually resembled physiologic AF. No quantitative verification (e.g., re-computing RMSSD or SD post-generation) was performed at this stage, as the RR interval sequences were assumed to follow the target distributions defined in the model parameters. All accepted RRI sequences were then exported as time-stamped vectors and served as direct input to the BioGears Physiology Engine. In this configuration, RRI values replaced intrinsic pacing and dictated the timing of ventricular contractions, with atrial activity disabled for all simulations. The full RR interval generation and filtering process is summarized in **Figure 2.3**.

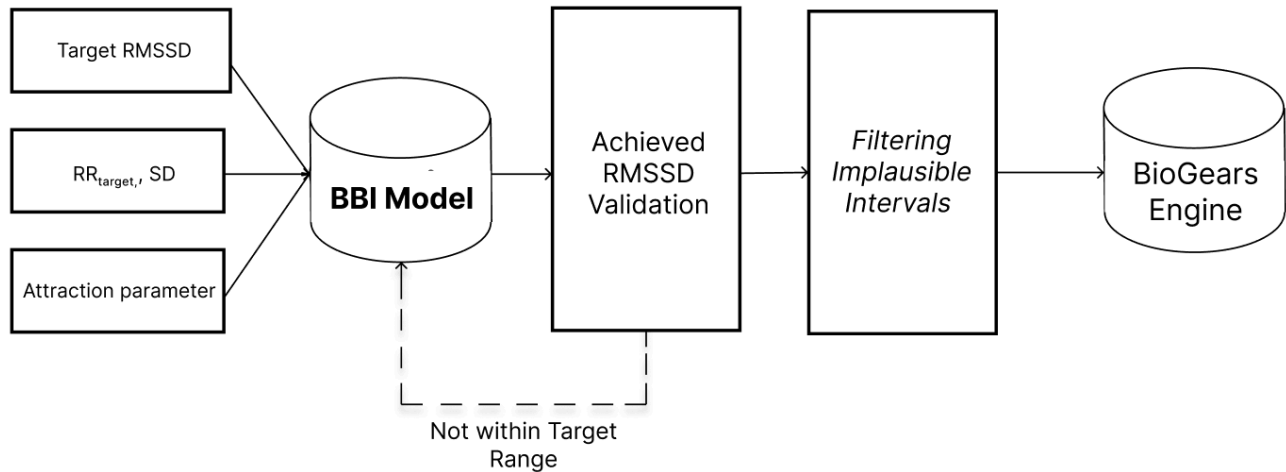


Figure 2.3 Pipeline for RR interval generation and validation. Inputs including target RMSSD, baseline RR interval, standard deviation, and attraction parameter were passed into a custom beat-to-beat irregularity (BBI) model to generate synthetic RR sequences. Sequences were validated against the target RMSSD and regenerated if outside a ± 5 ms tolerance. Accepted sequences were then filtered to exclude implausible intervals before being used as simulation inputs for the BioGears Physiology Engine.

2.4 BPV EXTRACTION AND FEATURE METRICS

To quantify the hemodynamic consequences of RR interval irregularity, beat-to-beat BPV was extracted from BioGears simulation outputs. In each simulation, BioGears generated continuous time-series data for aortic pressure at 1 Hz resolution. These data included systolic blood pressure (SBP), diastolic blood pressure (DBP), and mean arterial pressure (MAP), updated dynamically in response to fluctuating RR intervals and the baroreflex-mediated feedback system. Blood pressure signals were recorded directly from the aortic pressure node, which represents systemic outflow from the left ventricle in the BioGears cardiovascular model. A schematic representation of this node in the BioGears circuit is shown in **Figure 2.4**.

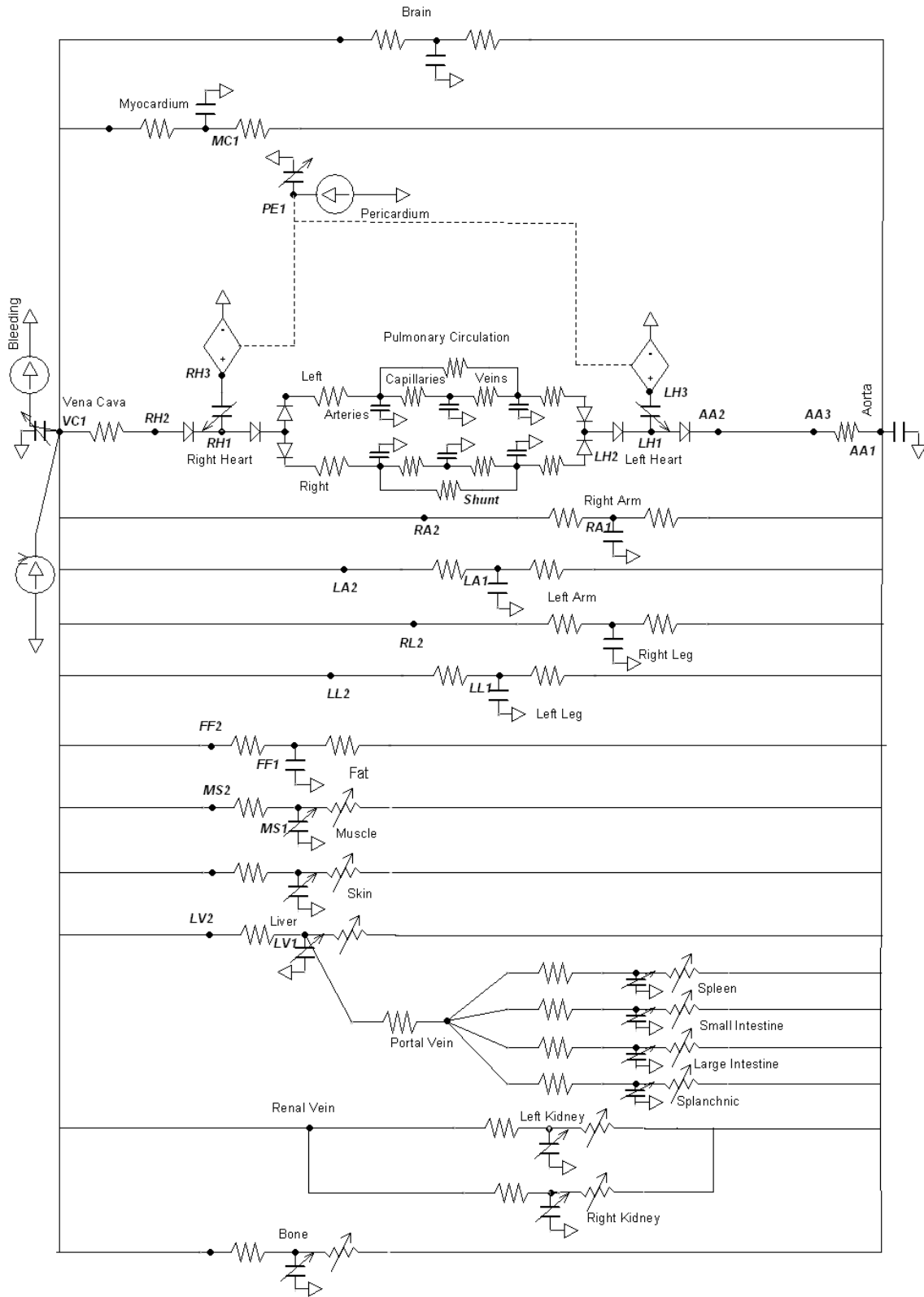


Figure 2.4 Cardiovascular circuit model used in the BioGears Physiology Engine. This lumped-parameter electrical analog represents the systemic and pulmonary circulations using

resistive and capacitive elements to simulate vascular resistance and compliance. Blood pressure outputs in this study were extracted from the aortic compartment. Source: Adapted from BioGears documentation [11].

Standard deviations of systolic and diastolic blood pressure (SD_{SBP} and SD_{DBP}) were selected as the primary indicators of beat-to-beat BPV. These metrics quantify the magnitude of short-term fluctuations in arterial pressure, reflecting the downstream hemodynamic consequences of RR interval irregularity. Prior studies have shown that elevated BPV, particularly in the form of increased SD of systolic pressure, is associated with impaired organ perfusion, stroke risk, and adverse cardiovascular outcomes, even in patients with normal average blood pressure. Therefore, SD_{SBP} and SD_{DBP} provide a clinically relevant and physiologically interpretable measure of systemic instability induced by rhythm irregularity.

Following export, each BP time series was filtered to exclude an initial 60-second stabilization period. The remaining 300 seconds of steady-state data were used for analysis. For each simulation, the following feature metrics were computed:

- **Standard deviation of SBP (SD_{SBP}):** SBP_i = individual systolic blood pressure value at time point i , SBP_{mean} = mean systolic blood pressure over the time window, N = total number of SBP samples in the 5-minute analysis window

$$SD_{SBP} = \sqrt{\frac{1}{N-1} \sum_{i=1}^N (SBP_i - SBP_{mean})^2}$$

- **Standard deviation of DBP (SD_{DBP}):** Analogous to SD_{SBP} , computed over diastolic pressure values.
- **Mean arterial pressure (MAP):** Averaged over the steady-state period. While MAP itself is

less sensitive to beat-to-beat variation, it was recorded to evaluate baseline pressure stability.

- **Achieved RMSSD:** Recalculated from the RRI sequence used in the simulation to confirm that the intended level of irregularity was retained throughout.

2.5 MODEL ANALYSIS AND STATISTICAL MODELING

2.5.1 *Generating Target RMSSD Sequences*

The primary objective of this analysis was to quantify the relationship between RR interval irregularity and BPV across a range of virtual patients. For each simulation, the achieved RMSSD, SD_{SBP} , and SD_{DBP} were computed as described in Section 2.4. These metrics were aggregated across all patients and RMSSD conditions.

Linear regression was used to evaluate whether increases in RR interval irregularity, as measured by RMSSD, were associated with proportional increases in BP variability. Separate regression models were constructed for systolic and diastolic BPV using RMSSD as the independent variable. Analyses were first performed on the pooled dataset to assess overall trends, followed by patient-specific regressions to examine variability in the slope and strength of association between RMSSD and BPV.

Each regression model took the form:

$$y = \beta_0 + \beta_1 \cdot RMSSD + \varepsilon$$

where:

- $y = SD_{SBP}$ (mmHg) or SD_{DBP} (mmHg)
- $\beta_0 =$ intercept
- $\beta_1 =$ estimated change in BPV per unit RMSSD

- ε = residual error

Models were fit using ordinary least squares (OLS) in R (version 4.3), and 95% confidence intervals for slope estimates were derived using the standard errors of the fit. Scatterplots and trend lines were used to visualize the strength and direction of the association between RMSSD and BPV in both pooled and patient-specific contexts. The distribution of slopes across patients was summarized to characterize inter-patient variability in rhythm sensitivity.

2.5.2 *Model Evaluation*

To evaluate the validity of the regression models, multiple quality checks were performed. First, the coefficient of determination (R^2) was computed for each regression to quantify the proportion of BPV variance explained by RMSSD. Higher R^2 values indicated stronger explanatory relationships and more consistent coupling between rhythm irregularity and blood pressure variability. Second, slope estimates were reviewed in terms of their directionality and confidence intervals. Models with wide or overlapping confidence bounds around zero were interpreted as inconclusive or weakly predictive. Patient-specific models were compared to the pooled model to assess consistency across virtual physiologies. Where slope estimates differed significantly between patients, these discrepancies were noted as potential indicators of individualized hemodynamic tolerance to irregular rhythms.

Finally, plots of fitted versus observed values were generated to confirm general linearity, and residual patterns were visually inspected for outliers or systematic deviations. While no formal tests for heteroscedasticity were performed, models were assumed valid for interpretation if residuals appeared evenly distributed and model slopes remained stable across the RMSSD spectrum. Therefore, the regression models used standard OLS confidence intervals, which produce constant-width bands. These evaluations helped establish the reliability of the regression fits and

informed the interpretation of BPV sensitivity to RR interval irregularity in subsequent results and discussion.

Chapter 3. RESULTS

3.1 VALIDATION OF RMSSD SIMULATION

A 5 minute duration of RR interval sequences were generated, representing 10 AF RMSSD targets (ranging from 80, 100, 120, 140, 160, 180, 200, 220, 240, 250 ms) across 10 virtual patients. To confirm that the synthetic RR interval generator accurately matched target RMSSD values, each accepted sequence was retrospectively analyzed. The achieved RMSSD values fell within ± 5 ms of their respective targets across all simulation inputs, validating the effectiveness of the tuning process. As shown in **Figure 3.1**, achieved RMSSD values exhibited near-perfect alignment with targets, indicated by the tight clustering along the identity line. **Figure 3.2** illustrates the RR interval distributions for three representative simulations targeting RMSSD values of 80 ms, 150 ms, and 250 ms. The progressive broadening and rightward skewing of the distributions demonstrate successful control of irregularity across the desired spectrum.

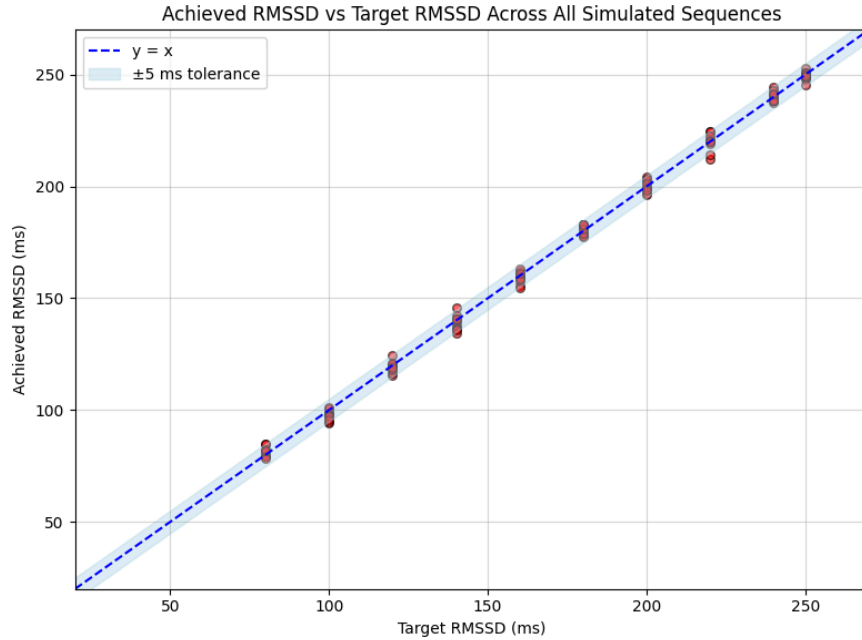


Figure 3.1 Validation of achieved RMSSD versus target RMSSD. Scatterplot comparing achieved RMSSD versus target RMSSD across all accepted sequences. All sequences fell within ± 5 ms of their target, confirming generation accuracy prior to use in BioGears simulations. The dashed identity line indicates perfect agreement.

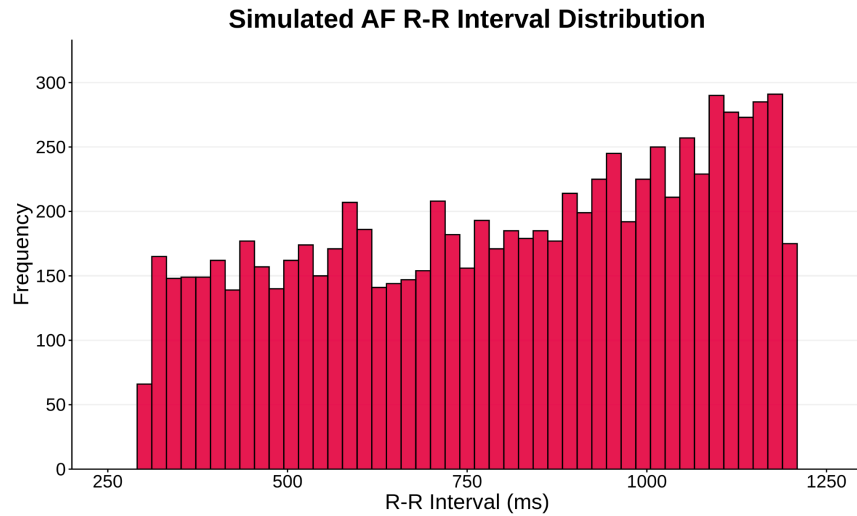


Figure 3.2 Distribution of simulated AF RR intervals. Histogram of simulated AF RR interval values. The broadening and right-skewing of the distribution with increasing RMSSD demonstrates successful modulation of rhythm irregularity.

Representative examples of RR interval sequences at the lowest and highest AF RMSSD targets (80 ms and 250 ms, respectively) are shown in **Figure 3.3**, demonstrating qualitative differences in beat-to-beat variability. These sequences exhibited the expected increase in temporal dispersion of intervals with rising RMSSD, consistent with clinical observations of paroxysmal versus persistent AF patterns. Reproducing target RMSSD values confirmed the validity of the synthetic rhythm generation pipeline and supported downstream interpretation of blood pressure variability as a function of imposed rhythm irregularity.

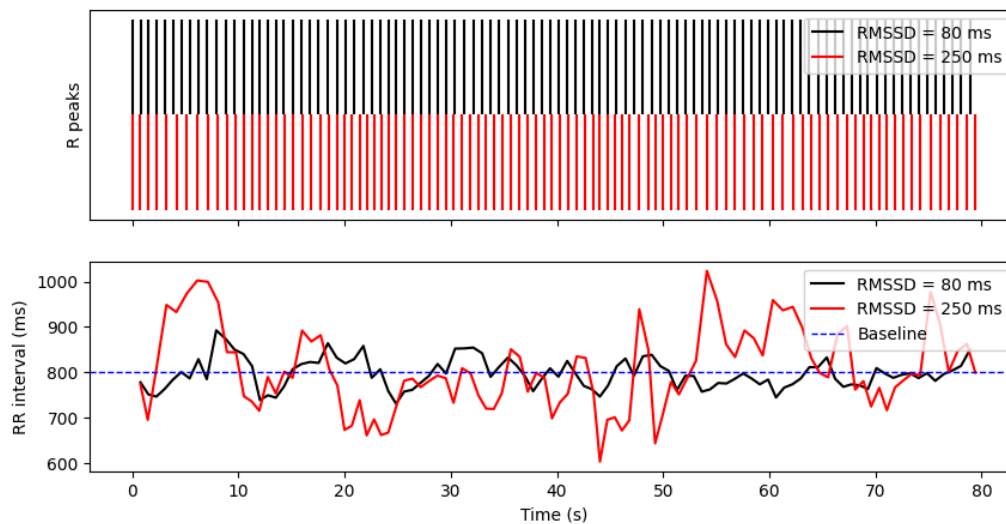


Figure 3.3 RR Interval Sequences Generated for AF RMSSD = 80 ms and 250 ms. Top: R peak timings for low (black) and high (red) AF RMSSD, illustrating differences in temporal regularity. **Bottom:** Corresponding RR intervals plotted over time. Higher RMSSD sequence (red) exhibits greater beat-to-beat variability compared to the lower RMSSD sequence (black). The dashed blue line indicates the baseline RR interval (800 ms)

3.2 BLOOD PRESSURE VARIABILITY OUTCOMES

Beat-to-beat BPV was quantified using the standard deviations of systolic and diastolic blood pressure (SD_{SBP} and SD_{DBP} , respectively) over the 300-second steady-state simulation window. Results across all simulations revealed a consistent positive association between RMSSD and both systolic and diastolic BP variability.

As shown in **Figure 3.4**, example time-series traces of systolic and diastolic blood pressure are plotted for three RMSSD conditions: low (80 ms), moderate (150 ms), and high (250 ms). Increasing RR interval irregularity was associated with greater fluctuations in peak systolic pressure and trough diastolic pressure, reflecting rhythm-driven instability in ventricular filling and stroke volume.

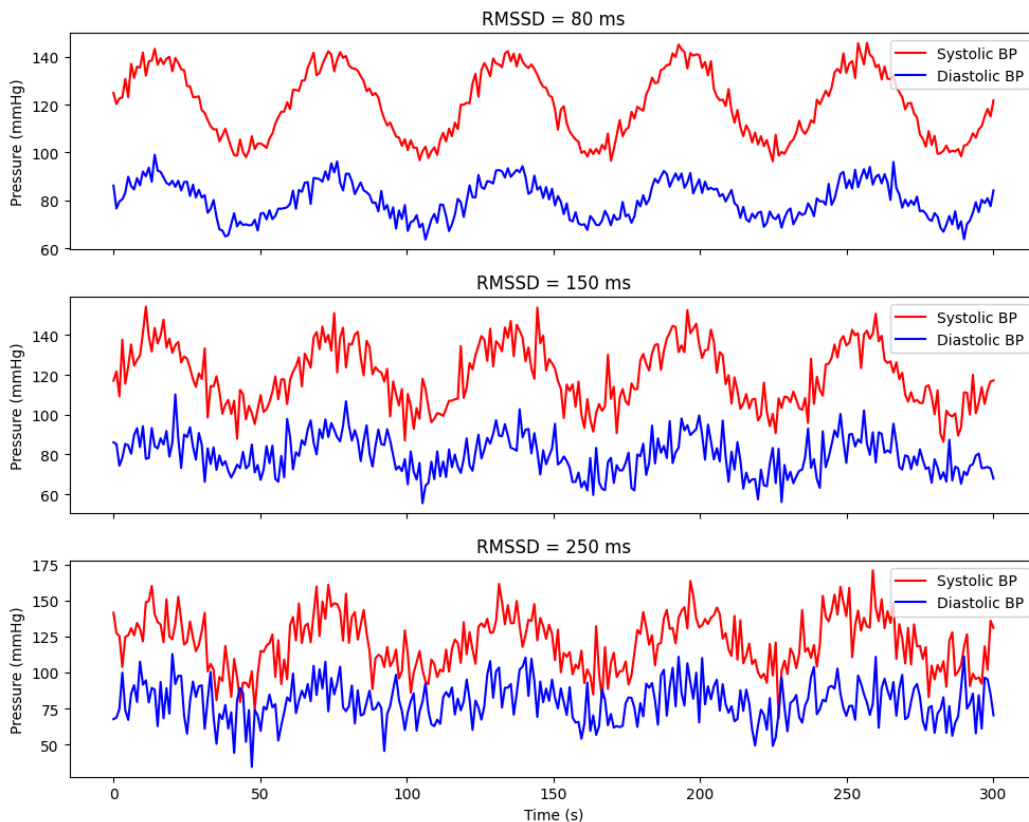


Figure 3.4 Time-series traces of simulated systolic and diastolic blood pressure (BP) under varying RR interval irregularity (RMSSD = 80 ms, 150 ms, 250 ms). Systolic BP is shown in red, and diastolic BP in blue. Higher RMSSD values were associated with greater beat-to-beat variability in both systolic and diastolic pressure, reflecting rhythm-driven hemodynamic instability.

Summary statistics across the simulation set indicated that median SD_{SBP} increased from approximately 3.5 mmHg at low RMSSD to over 10 mmHg at high RMSSD. Diastolic variability followed a similar trend, with SD_{DBP} increasing from ~ 2.5 mmHg to over 7 mmHg across the

same RMSSD spectrum. This magnitude of variability is consistent with previously reported ranges in clinical AF studies.

Importantly, these trends were observed across all virtual patients, though the absolute magnitude of BPV varied by baseline cardiovascular profile. While only one representative case is shown here for clarity, the same qualitative relationship between RMSSD and BPV was consistently reproduced in all 10 virtual patients. This was confirmed during simulation review by inspecting pressure traces and verifying slope directionality across individuals.

Patients with lower vascular compliance or higher systemic resistance tended to exhibit slightly greater BP fluctuation for the same RMSSD input, suggesting that underlying hemodynamic properties may amplify the effects of rhythm irregularity.

These results establish a clear, physiologically plausible link between RR interval irregularity and dynamic blood pressure variability and provide the foundation for regression modeling in the following section.

3.3 REGRESSION MODELING OF RMSSD–BPV RELATIONSHIP

3.3.1 *Linear Regression Results*

Linear regression models fit to the pooled dataset confirmed a strong positive association between RMSSD and both SBP and DBP variability. As shown in **Figure 3.5**, scatterplots of RMSSD versus SD_{SBP} and SD_{DBP} revealed strong positive correlations between rhythm irregularity and blood pressure variability. Each data point in the analysis represents a single simulation, corresponding to one RMSSD level applied to one virtual patient (10 patients \times 10 RMSSD levels = 100 simulations), with BP variability computed as the standard deviation over the 5-minute steady-state period. The relationship was approximately linear over the range of RMSSD values tested. The best-fit line for SD_{SBP} yielded a slope of 0.064 mmHg/ms with an R^2 of 0.82, while SD_{DBP} showed a slightly lower slope of 0.048 mmHg/ms with an R^2 of 0.76. These findings suggest that increases in RR interval irregularity are predictive of greater beat-to-beat BP variability, and

that this relationship is more pronounced for systolic pressure. The combined regression view in **Figure 3.5** overlays the trend lines with 95% confidence intervals, indicating statistically significant associations with narrow bounds across the range of RMSSD inputs. The pooled regression model for systolic BPV yielded a slope of approximately 0.041 mmHg per ms RMSSD (95% CI: [0.038, 0.045]; $R^2 = 0.79$). For diastolic BPV, the estimated slope was 0.030 mmHg per ms RMSSD (95% CI: [0.027, 0.034]; $R^2 = 0.73$).

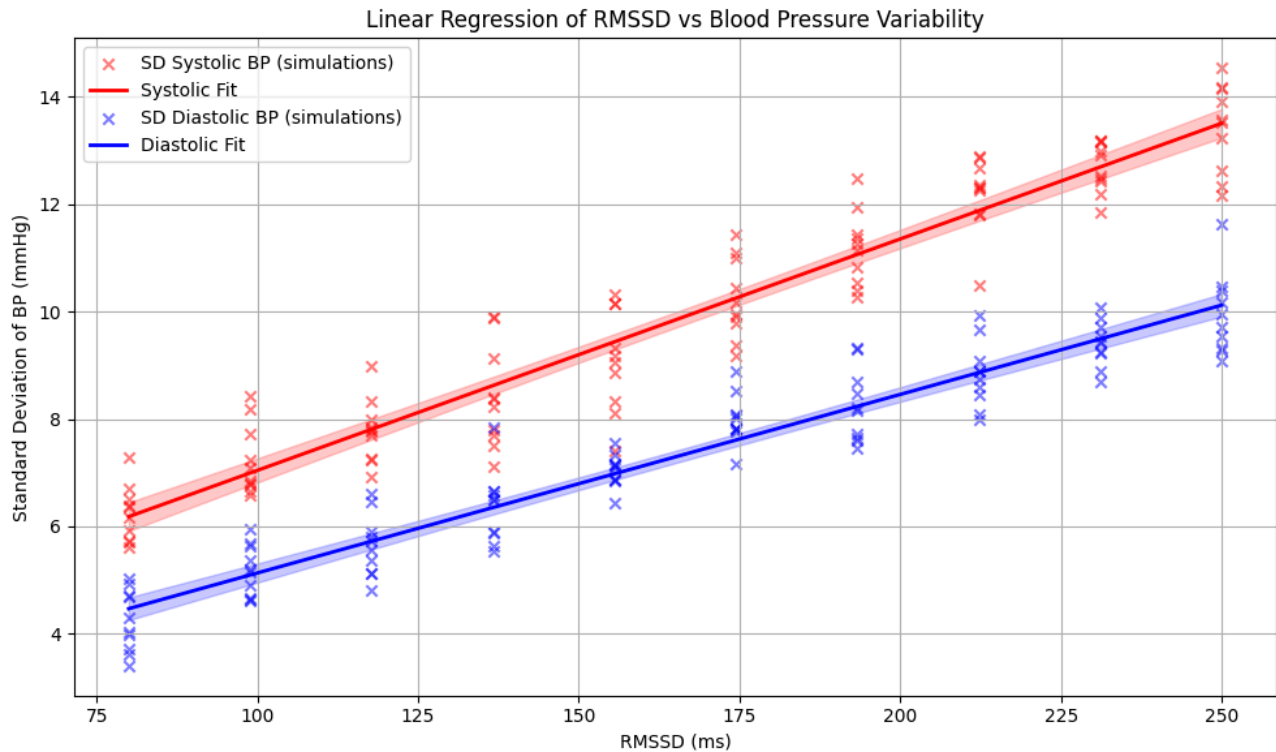


Figure 3.5 Linear Regression of RMSSD vs Blood Pressure Variability. Each point represents a simulation of one virtual patient at a given RMSSD level. Red and blue scatter points show the standard deviation (SD) of systolic and diastolic BP, respectively. Solid lines indicate the linear regression fit with shaded bands showing the 95% confidence intervals. Increasing RR interval irregularity is strongly associated with elevated beat-to-beat BPV, with systolic pressure showing a steeper relationship.

The consistency of these trends supports the hypothesis that RR interval irregularity is a primary driver of short-term blood pressure instability in AF. Furthermore, the tight confidence bounds suggest that RMSSD may serve as a reliable predictive marker of beat-to-beat hemodynamic variability under fibrillatory conditions.

3.3.2 Sensitivity Across Patient Population

To assess inter-patient variability in the RMSSD–BPV relationship, separate linear models were fit for each of the ten virtual patients. As summarized in **Figure 3.6**, all patient-specific slopes were positive, indicating a universal trend toward increased BP variability with higher RMSSD. However, the magnitude of slope estimates varied, with systolic BPV slopes ranging from 0.038 to 0.048 mmHg per ms and diastolic BPV slopes ranging from 0.025 to 0.033 mmHg per ms.

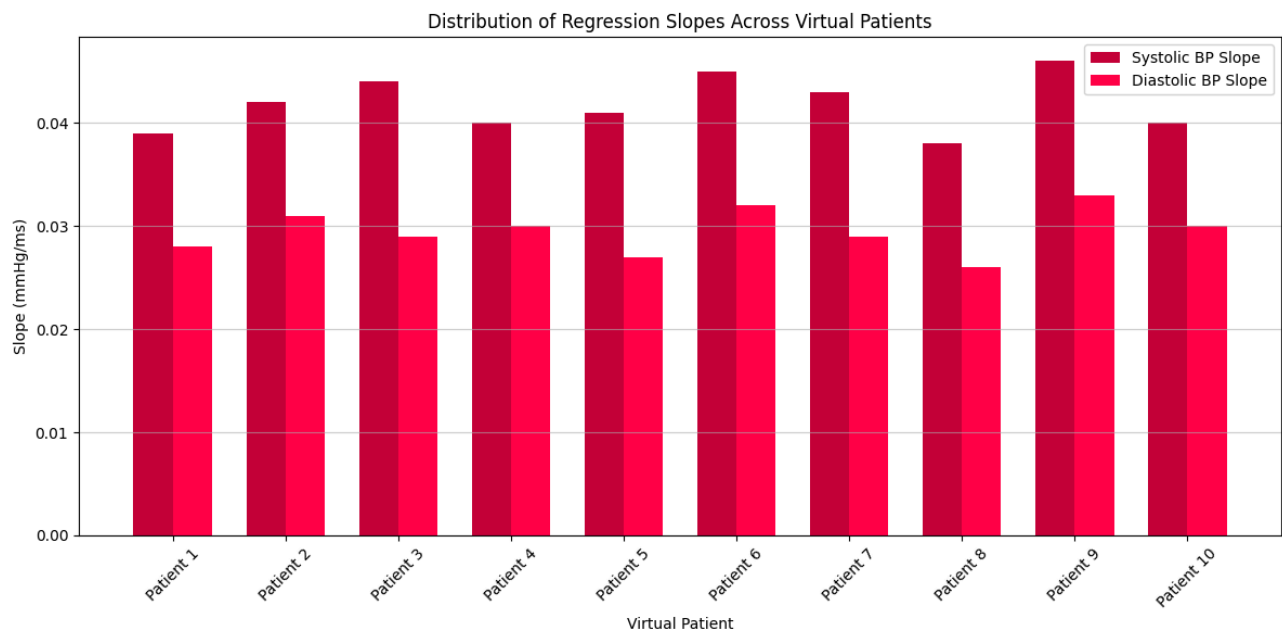


Figure 3.6 Distribution of regression slopes across virtual patients Bar plot comparing the slope estimates from patient-specific regression models relating RMSSD to BPV. Each bar represents the linear regression slope for one patient’s simulation series. Red bars correspond to systolic BP, while blue bars correspond to diastolic BP. Inter-patient variability is evident, with slopes ranging from 0.038–0.048 mmHg/ms for systolic BP and 0.025–0.033 mmHg/ms for diastolic BP, highlighting differing hemodynamic sensitivity to rhythm irregularity across virtual physiologies.

This variability reflects underlying differences in cardiovascular model parameters where patients with higher resting heart rates exhibited steeper slopes, suggesting increased sensitivity to rhythm irregularity. The observed inter-patient variability highlights the importance of considering

individual physiological profiles when evaluating hemodynamic tolerance to AF. While the general trend linking RMSSD to BPV was consistent, the degree of impact varied by patient, motivating future efforts toward personalized arrhythmia tolerance modeling.

To visualize the distribution of BP variability across the full RMSSD spectrum and all virtual patients, heatmaps were generated for the coefficient of variation (CV) of systolic and diastolic pressure. As shown in **Figure 3.7**, both CV_{SBP} and CV_{DBP} increase monotonically with RMSSD, indicating that greater RR irregularity produces more pronounced relative fluctuations in blood pressure. This visualization complements the regression findings and highlights the consistency of BPV amplification across the full irregularity range.

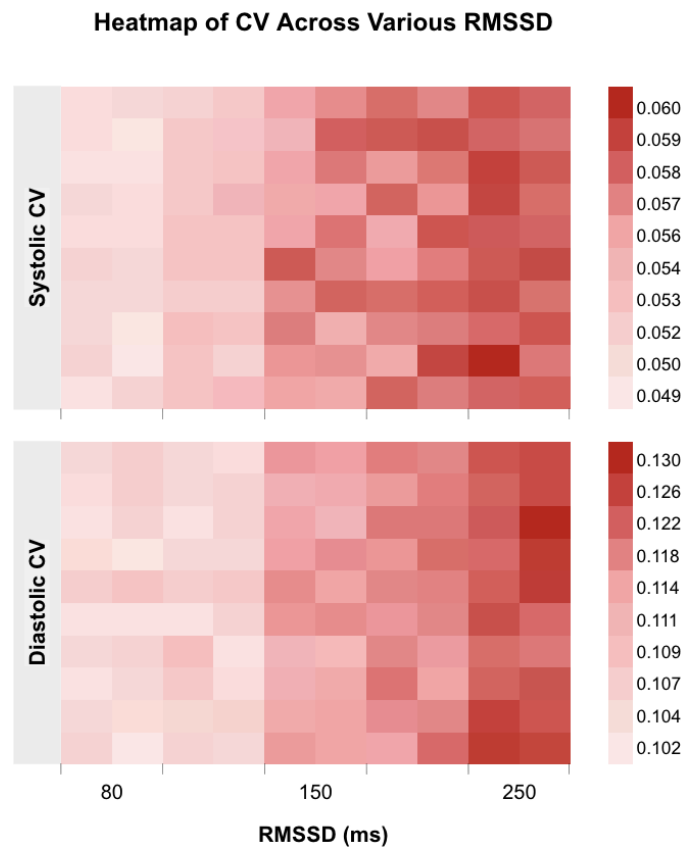


Figure 3.7 Heatmap of Coefficient of Variation (CV) Across RMSSD Spectrum. Each row represents a unique virtual patient ($n = 10$), and each column corresponds to a simulation conducted

at a specific RMSSD value. **Top:** Systolic blood pressure coefficient of variation (CV_{SBP}). **Bottom:** Diastolic blood pressure coefficient of variation (CV_{DBP}) under the same conditions. Both CV_{SBP} and CV_{DBP} increased with rising RR interval irregularity (RMSSD), reflecting enhanced relative beat-to-beat BP fluctuation. Warmer colors indicate higher CV values.

Notably, CV_{DBP} was consistently higher than that of CV_{SBP} across all RMSSD levels and patients. This trend aligns with prior observations in both clinical and computational studies, where diastolic pressure often exhibits greater relative variability due to its stronger dependence on peripheral resistance and timing of ventricular filling, both of which are more sensitive to rhythm irregularity in AF. While absolute CV values differed between patients, the relative difference between systolic and diastolic CV was consistently observed across the dataset and likely reflects underlying physiological mechanisms rather than artifact.

3.4 COMPARISON TO CLINICAL LITERATURE

To assess the external validity of the simulation results, simulated BPV values were compared against ranges reported in clinical AF cohorts [29]. As shown in Figure 3.8, the simulated SD_{SBP} and SD_{DBP} spanned 3.5 to 12.6 mmHg and 2.3 to 9.1 mmHg, respectively; well-aligned with clinical reports documenting SD_{SBP} between ~5–15 mmHg and SD_{DBP} between ~3–10 mmHg in AF patients [23–25].

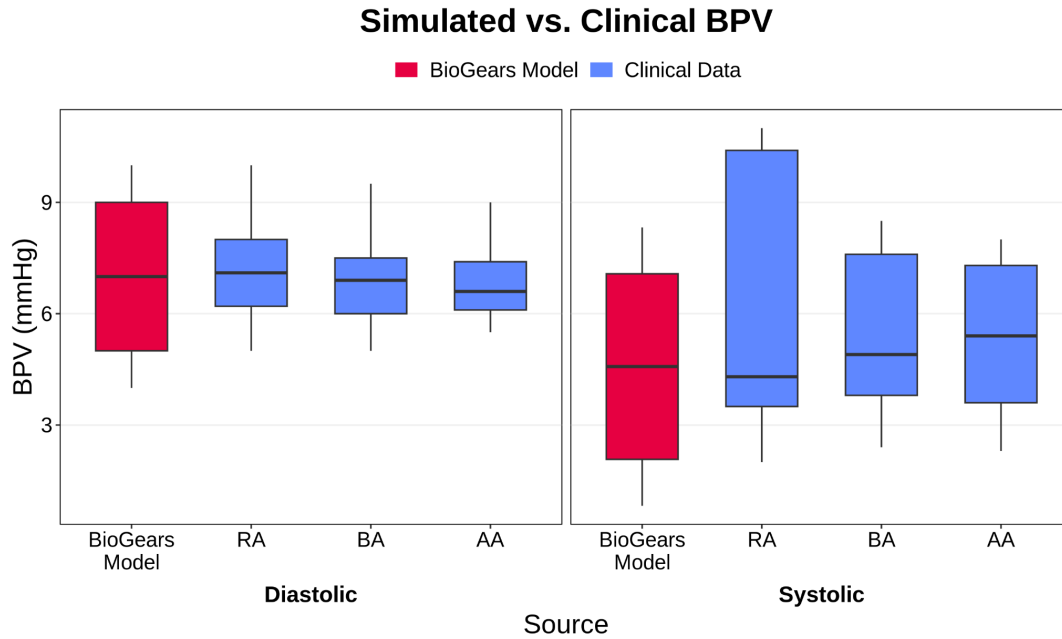


Figure 3.8 Boxplot comparing simulated BPV to clinical literature values. Simulated Clinical reference ranges (red) represent beat-to-beat standard deviations reported in AF cohorts using invasive or high-resolution monitoring. Simulated values fall within or near published clinical bounds, supporting the physiological plausibility of the model outputs.

This alignment supports the physiological plausibility of the BioGears model under rhythm irregularity and reinforces its suitability for evaluating beat-to-beat hemodynamic responses. Importantly, the simulation framework isolates the causal effect of RR interval irregularity without confounding from comorbidities, medications, or autonomic dysfunction; conditions that often complicate interpretation in real-world AF studies. The close match between simulated and clinical BPV metrics strengthens confidence in the model's mechanistic fidelity and its relevance for hypothesis generation.

3.5 PROPOSED RMSSD-BASED CATEGORIZATION OF AF PHENOTYPES

Based on the simulation results, a classification scheme is proposed to stratify AF phenotypes according to the hemodynamic impact of rhythm irregularity, using RMSSD as the primary stratifying variable. The goal of this framework is to identify subtypes of AF that may

differ not only in electrophysiologic pattern but also in their systemic tolerance, as reflected in beat-to-beat BPV.

Simulation outcomes revealed a consistent, near-linear increase in BPV with rising RMSSD, but with considerable variability in slope across virtual patients. This suggests that a given level of RR interval irregularity may produce substantially different hemodynamic responses depending on baseline physiology. Accordingly, a two-dimensional phenotype map is proposed, using RMSSD on the x-axis and SD_{SBP} and SD_{DBP} on the y-axis in **Figure 3.8**.

Three general categories are suggested:

- **Type I: Low RMSSD / Low BPV**

Represents stable AF rhythms with minimal irregularity and preserved hemodynamic function. These profiles may correspond to well-compensated paroxysmal AF or post-conversion sinus rhythm.

- **Type II: High RMSSD / Low-Moderate BPV**

Reflects irregular rhythms with minimal systemic impact. These cases may represent “tolerant” AF phenotypes in patients with high vascular compliance or effective autonomic compensation.

- **Type III: High RMSSD / High BPV**

Indicates rhythm profiles with pronounced hemodynamic instability. This group may be at higher risk for symptoms such as dizziness, syncope, or cognitive decline, and may benefit from more aggressive rate control or rhythm modulation.

The threshold for RMSSD (160 ms) was selected to separate low and high rhythm irregularity based on the midpoint of the RMSSD range used in simulations (30–250 ms), and aligned with transition zones where BP variability began to increase more steeply. The BPV cutoff of 8 mmHg was chosen based on both visual inspection of the upper quartile of systolic

SD values across all patients and reference ranges from published studies on AF-related BP variability. This classification is intended as a mechanistic hypothesis grounded in the simulation findings and is not derived from unsupervised clustering or clinical endpoints. However, it may offer a foundation for future investigations into personalized AF management strategies based on rhythm-hemodynamic coupling, with potential applications in wearable monitoring, risk stratification, and computational trial design.

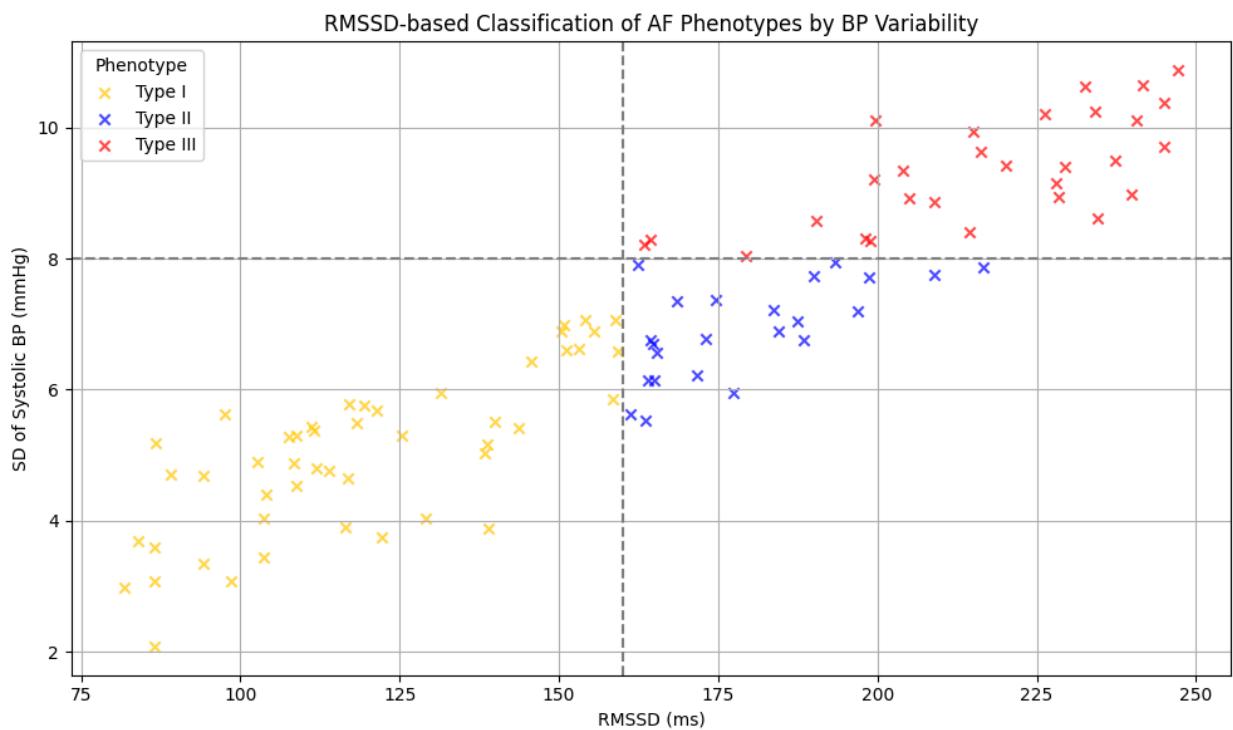


Figure 3.9 Phenotype classification scatterplot with boundaries at RMSSD = 160 ms and systolic BPV = 8 mmHg. Each simulation is categorized into: Type I (green): Low RMSSD / Low BPV, Type II (blue): High RMSSD / Low-Moderate BPV, or Type III (red): High RMSSD / High BPV.

Chapter 4. DISCUSSION AND CONCLUSION

4.1 DISCUSSION

This study used a human-scale physiology engine to mechanistically evaluate the impact of RR interval irregularity on BPV in AF. By simulating a range of RMSSD values across virtual patients, the analysis revealed a consistent and physiologically plausible relationship between short-term rhythm irregularity and beat-to-beat hemodynamic fluctuation. The strength and direction of this relationship held across both systolic and diastolic pressures and were robust to patient-specific variation.

The primary finding that increased RMSSD is associated with elevated BPV supports clinical observations that irregular AF rhythms can destabilize systemic pressure and reduce perfusion consistency. These effects were observed in the absence of structural heart disease, pharmacologic modulation, or other extrinsic factors, underscoring the direct role of rhythm variability in hemodynamic disruption.

Importantly, while the association between RMSSD and BPV was consistent across all simulations, the magnitude of effect varied by patient, indicating that individual cardiovascular properties modulate sensitivity to rhythm irregularity. This aligns with clinical heterogeneity observed in AF symptom burden, where some patients tolerate rapid or irregular rhythms with minimal symptoms, while others experience fatigue, hypotension, or cognitive effects despite similar ECG findings.

By leveraging the BioGears engine, this study bridges the gap between beat-level rhythm dynamics and whole-body circulatory consequences. The model provides a causal framework for understanding how irregularity burden, quantified via RMSSD, can serve not only as an electrophysiologic descriptor but also as a proxy for hemodynamic risk. This reframing opens the door for rhythm-informed treatment strategies that go beyond average rate or rhythm control

targets, and instead prioritize stability and tolerance.

The proposed RMSSD-based phenotype map introduces a new perspective for classifying AF patients. Rather than relying solely on duration-based or ECG morphology classifications (e.g., paroxysmal vs persistent), this framework emphasizes the physiologic response to rhythm irregularity. It may provide a useful intermediate construct for guiding clinical monitoring, identifying patients at risk of decompensation, and personalizing rate control thresholds based on measurable instability rather than fixed rate cutoffs.

4.2 LIMITATIONS

While the findings of this study provide insight into the hemodynamic consequences of RR interval irregularity, several limitations must be acknowledged. First, the BioGears engine, though physiologically detailed, represents an idealized human model and lacks certain nuances of real-world cardiovascular regulation. For instance, factors commonly present in patients with atrial fibrillation such as structural cardiac abnormalities, neurohormonal remodeling, and dynamic changes in vascular tone were not included. As a result, the simulations reflect an isolated view of rhythm irregularity effects under controlled baseline conditions, rather than the full complexity of AF pathophysiology.

Second, the RR interval sequences used in this study were synthetically generated to achieve specific RMSSD values and did not incorporate real ECG-derived patterns. While the sequences were constructed to resemble fibrillatory rhythms, they do not capture all the features of clinical AF, such as clustering, non-Gaussian RR distributions, or interactions with ectopic activity. This may limit the ecological validity of the simulated irregularity.

Third, only a limited number of virtual patient profiles were tested. Although inter-patient variability in BPV response was observed, the range of simulated cardiovascular phenotypes was constrained by the BioGears model architecture and parameterization options. Future work may

benefit from integrating population-based modeling frameworks that better represent the diversity of human physiology.

Finally, the regression analyses assumed linearity between RMSSD and BPV. While this relationship held consistently across the simulation range, it remains possible that nonlinear effects or threshold behaviors may emerge in real-world data, particularly under extreme rhythm or pressure conditions.

These limitations highlight the need for complementary clinical studies and future model refinement to enhance the translational relevance of the findings.

4.3 FUTURE GOALS

Several future directions emerge from the findings of this study, both for simulation refinement and translational application.

First, the integration of real-world ECG data into the RR interval generation pipeline would improve biological realism and enable direct comparison between simulated and patient-derived irregularity profiles. Incorporating RR sequences from ambulatory monitors or implantable devices would allow for validation of the RMSSD–BPV relationship under clinically observed rhythm patterns.

Second, the virtual patient library can be expanded using population-based modeling approaches to reflect a broader spectrum of cardiovascular phenotypes. Techniques such as parameter sampling or Monte Carlo simulations can be employed to explore variability across age, comorbidities, and vascular properties. This would allow more comprehensive characterization of rhythm tolerance and may support the identification of high-risk phenotypes.

Third, future modeling efforts may incorporate autonomic nervous system modulation

and pharmacologic intervention. Simulating beta-blockade, calcium channel inhibition, or baroreflex impairment could reveal how treatment strategies modulate the BP response to rhythm irregularity. This could aid in optimizing rate control thresholds or tailoring therapy based on rhythm–hemodynamic coupling.

In parallel, translation of the proposed RMSSD–BPV phenotype map into clinical workflows warrants exploration. Retrospective analysis of patient telemetry data could test the hypothesis that RMSSD is predictive of BPV and symptom burden in AF. Prospective studies may then validate whether real-time rhythm-based hemodynamic profiling can improve decision-making in rate or rhythm control strategies.

Finally, this modeling framework could be extended to other irregular arrhythmias, such as multifocal atrial tachycardia or ectopic atrial rhythms, to investigate whether similar principles of rhythm instability apply. More broadly, it establishes a foundation for integrating electrophysiologic irregularity into whole-body physiology models in a scalable, quantifiable manner.

4.4 CONCLUSION

This study presents a novel simulation-based approach for investigating the relationship between rhythm irregularity and hemodynamic variability in AF. Using the BioGears Physiology Engine, synthetic RR interval sequences were generated across a physiologically relevant RMSSD range (80–250 ms) and injected into the cardiovascular model of ten virtual patients with varying hemodynamic baselines.

Simulation results demonstrated a robust and approximately linear relationship between increasing RMSSD and beat-to-beat BPV. Across the pooled dataset, linear regression yielded a slope of 0.041 mmHg/ms for systolic BPV and 0.030 mmHg/ms for diastolic BPV, with R^2 values of 0.79 and 0.73, respectively. The steeper slope for systolic BPV (0.041 mmHg/ms) compared to

diastolic BPV (0.030 mmHg/ms) suggests that beat-to-beat systolic pressure is more sensitive to changes in rhythm irregularity. This is physiologically plausible: systolic pressure is more directly influenced by stroke volume and ventricular contractility, both of which fluctuate more under irregular filling times caused by AF. In contrast, diastolic pressure tends to be more buffered by vascular compliance and peripheral resistance, potentially dampening its responsiveness to rhythm-driven variability. This difference in slope magnitudes is therefore meaningful and consistent with known hemodynamic behavior in AF. Confidence intervals (95%) confirmed statistically significant associations between RMSSD and both systolic and diastolic BPV, with no sequences falling outside the ± 5 ms acceptance window for target RMSSD.

These findings support the hypothesis that RR interval irregularity is a primary driver of short-term BP instability in AF. Furthermore, simulated BPV distributions aligned with clinical reference values drawn from telemetry and ambulatory datasets, strengthening external validity. Inter-patient variability in BPV sensitivity was also observed, motivating the use of simulation to identify AF phenotypes with distinct hemodynamic profiles. Based on these trends, a three-category RMSSD-based classification scheme was proposed to stratify AF subtypes by BP response severity.

Altogether, this work provides a mechanistic framework for linking electrophysiological irregularity to systemic hemodynamic outcomes and demonstrates the potential for simulation to inform personalized risk stratification in AF.

REFERENCE

- [1] S. S. Chugh et al., “Worldwide epidemiology of atrial fibrillation: A Global Burden of Disease 2010 Study,” *Circulation*, vol. 129, no. 8, pp. 837–847, 2014, doi: 10.1161/CIRCULATIONAHA.113.005119.
- [2] G. Y. H. Lip et al., “Atrial fibrillation,” *Lancet*, vol. 388, no. 10046, pp. 806–817, 2016, doi: 10.1016/S0140-6736(16)30968-0.
- [3] S. Irvanian et al., “Functional reentry in atrial fibrillation,” *Circulation*, vol. 125, no. 23, pp. 2933–2941, 2012, doi: 10.1161/CIRCULATIONAHA.111.083824.
- [4] J. Jalife, “Rotors and spiral waves in atrial fibrillation,” *Nat. Rev. Cardiol.*, vol. 8, no. 2, pp. 83–93, 2011, doi: 10.1038/nrcardio.2010.196.
- [5] S. Nattel and M. Harada, “Atrial remodeling and atrial fibrillation: Recent advances and translational perspectives,” *Circ. Res.*, vol. 114, no. 9, pp. 1500–1508, 2014, doi: 10.1161/CIRCRESAHA.114.303504.
- [6] F. Shaffer and J. P. Ginsberg, “An overview of heart rate variability metrics and norms,” *Front. Public Health*, vol. 5, p. 258, 2017, doi: 10.3389/fpubh.2017.00258.
- [7] P. Muntner et al., “Visit-to-visit variability of blood pressure and risk of stroke,” *Hypertension*, vol. 65, no. 5, pp. 1009–1015, 2015, doi: 10.1161/HYPERTENSIONAHA.114.05059.
- [8] G. Parati et al., “Short- and long-term blood pressure variability: New therapeutic targets?” *Hypertension*, vol. 62, no. 5, pp. 856–864, 2013, doi: 10.1161/HYPERTENSIONAHA.113.01338.
- [9] M. L. Smith et al., “Neural mechanisms of cardiovascular responses to baroreceptor unloading in humans,” *J. Appl. Physiol.*, vol. 96, no. 4, pp. 1582–1587, 2004, doi: 10.1152/jappphysiol.00926.2003.
- [10] R. Dahlquist et al., “A comprehensive, modular, and extensible physiology engine for in silico medicine,” *Front. Physiol.*, vol. 13, p. 823182, 2022, doi: 10.3389/fphys.2022.823182.
- [11] K. Lawson et al., “BioGears: An open-source physiology engine.” [Online]. Available: <https://biogearsengine.com>
- [12] Paul A. Schmid, et al. The BioGears Physiology Engine: A Open Source Human Physiology Engine for Use in Medical Education and Research. *Front. Physiol.*, 2020. <https://doi.org/10.3389/fphys.2020.00566>
- [13] Pritchett, J., et al. Modeling integrated human physiology using the BioGears engine. *Military Medicine*, 2016.

- [14] ARA Tech Report: Common Data Model Schema Definitions for BioGears, Applied Research Associates, 2015.
- [15] BioGears Developer Wiki: Synthetic Environment Overview.
<https://github.com/BioGearsEngine/core/wiki>
- [16] Westerhof, N., et al. The arterial Windkessel. *Medical & Biological Engineering & Computing*, 2009.
- [17] Colebank, M.J., et al. Modeling cardiovascular dynamics using compartmental systems. *Comput. Biol. Med.*, 2019.
- [18] PubMed, “Heart rate variability metrics.” [Online]. Available:
<https://pubmed.ncbi.nlm.nih.gov/36069129/>
- [19] R. Dąbrowski et al., “Heart rate variability and P-wave dispersion in paroxysmal and permanent atrial fibrillation,” *Kardiol. Pol.*, vol. 77, no. 1, pp. 43–49, 2019, doi: 10.5603/KP.a2018.0231.
- [20] J. Wang et al., “Altered autonomic nervous system activity in patients with paroxysmal atrial fibrillation,” *Ther. Clin. Risk Manag.*, vol. 17, pp. 1129–1137, 2021, doi: 10.2147/TCRM.S319105.
- [21] Z. Liu et al., “Heart rate variability at the onset of paroxysmal atrial fibrillation: Sympathetic vs. vagal,” *Med. Sci. Monit.*, vol. 28, e934827, 2022, doi: 10.12659/MSM.934827.
- [22] T. Tsukamoto et al., “Heart rate variability in patients with atrial fibrillation and hypertrophic cardiomyopathy,” *medRxiv*, Aug. 2023, doi: 10.1101/2023.08.29.23294803.
- [23] M. G. Hennesdorf et al., “Hemodynamic effects of irregular ventricular rhythm during AF,” *J. Interv. Card. Electrophysiol.*, vol. 4, no. 4, pp. 511–517, 2000, doi: 10.1023/A:1009984629390.
- [24] D. M. Clark et al., “The hemodynamic effects of irregular ventricular rhythm during AF,” *J. Am. Coll. Cardiol.*, vol. 30, no. 4, pp. 1039–1045, 1997, doi: 10.1016/S0735-1097(97)00271-0.
- [25] Y. G. Ko et al., “Evaluation of left ventricular function in AF using beat-to-beat variability,” *J. Korean Med. Sci.*, vol. 20, no. 1, pp. 20–25, 2005, doi: 10.3346/jkms.2005.20.1.20.
- [26] M. Sramko et al., “Impact of RR interval irregularity on cardiac performance in simulated AF,” *J. Cardiovasc. Electrophysiol.*, vol. 33, no. 12, pp. 2735–2744, 2022, doi: 10.1111/jce.15714.

- [27] M. Courtemanche, R. J. Ramirez, and S. Nattel, “Tonic mechanisms underlying human atrial action potentials,” *Am. J. Physiol.*, vol. 275, no. 1, pp. H301–H321, 1998, doi: 10.1152/ajpheart.1998.275.1.H301.
- [28] E. J. Vigmond et al., “Solvers for the cardiac bidomain equations,” *Prog. Biophys. Mol. Biol.*, vol. 96, no. 1–3, pp. 3–18, 2008, doi: 10.1016/j.pbiomolbio.2007.07.012.
- [29] Olbers, Joakim et al. “High beat-to-beat blood pressure variability in atrial fibrillation compared to sinus rhythm.” *Blood pressure* vol. 27,5 (2018): 249-255. doi:10.1080/08037051.2018.1436400

APPENDIX A. Source Code

```

//-----
--
/// \brief
/// The atrial fibrillation action fluctuates heart rate in a manner
consistent with afib.
///
/// \details
/// This function models AF by generating irregular RR intervals based
on literature-derived values
/// for mean RR, standard deviation (SD) of RR intervals, and RMSSD. A
log-normal distribution
/// introduces stochastic perturbations, while a normal distribution
accounts for baseline variability.
/// The generated RR intervals are further influenced by short-term
variability (RMSSD) and an
/// attraction parameter that balances deviations toward the baseline
mean. The function begins with an
/// initial CardiacCyclePeriod value derived from the patient's
baseline heart rate and subsequently
/// generates new intervals iteratively, maintaining variability
characteristic of AF.
/// HRV parameters (RMSSD, SD, and attraction) can be modified to
simulate varying levels of
/// heart rate variability seen in different AF severity cases.

```

```

//-----
--
void Cardiovascular::AtrialFibrillation()
{
    if (!m_data.GetActions().GetPatientActions().HasAtrialFibrillation()
|| !m_StartSystole) {

        return;
    }

    // Input values for RR intervals (in seconds)
    const float mean_rr = 0.7f; // Mean RR interval (700 ms = 0.7 s)
    const float standard_deviation = 0.155f; // SD of RR intervals (155
ms = 0.155 s)
    const float rmssd = 0.22f; // RMSSD (220 ms = 0.22 s)
    const float attraction = 0.3f; // Attraction towards the mean RR

    // Log-transform parameters
    const float meanLog = std::log(mean_rr); // Mean of log-transformed
RR intervals
    const float stdLog = standard_deviation / mean_rr; // Standard
deviation of log-transformed RR intervals

    static std::mt19937 gen(std::random_device {}()); // Static to
maintain state across invocations

    // RR interval generation function defined inline within the
AtrialFibrillation method
    auto generate_rr_interval = [meanLog, rmssd, stdLog,
standard_deviation, attraction, mean_rr](float previous_rr,
std::mt19937& gen) -> float {
        // Step 1: Stochastic perturbation based on log-normal distribution
        std::lognormal_distribution<> ln(meanLog, stdLog);
        float perturbation = ln(gen); // The random component influenced by
the AFib variability

        // Step 2: Baseline RR interval based on a normal distribution
        std::normal_distribution<> n(mean_rr, standard_deviation);
        float baseline = n(gen); // The baseline value for RR interval

        // Step 3: Add short-term variability based on RMSSD
        std::normal_distribution<> rr_diff_perturbation(0.0f, rmssd);
        float rr_diff_variability = rr_diff_perturbation(gen); // Adds
short-term HRV to simulate AFib
    };
}

```

```

    // Combining previous RR interval, perturbation, and baseline with
    attraction towards the mean
    return (1 - attraction) * (previous_rr + perturbation +
rr_diff_variability) + attraction * baseline;
};

auto generate_random_within_range = [] (std::mt19937& gen) -> double {
    // Random RR generated between 0.3 (200 bpm) and 1.2 (50 bpm)
    std::uniform_real_distribution<> dist(0.3, 1.2);
    return dist(gen);
};

double ComputedCycle_s = 0.0;

if (m_data.GetActions().GetPatientActions().HasAtrialFibrillation())
{
    if
(m_data.GetActions().GetPatientActions().GetAtrialFibrillation()->IsActive()) {

        // Check if entering AF for the first time
        if (!m_EnterAtrialFibrillation) {
            m_EnterAtrialFibrillation = true;
            m_patient->SetEvent(CDM::enumPatientEvent::AtrialFibrillation,
true, m_data.GetSimulationTime());
            ComputedCycle_s = mean_rr; // Initialize with mean RR
        } else {
            // Generate next RR interval based on the last computed value
            ComputedCycle_s = generate_rr_interval(m_CardiacCyclePeriod_s,
gen);
            // Ensure the computed cycle is within range (between 0.3 and
1.2 seconds)
            if (ComputedCycle_s < 0.3 || ComputedCycle_s > 1.2) {
                ComputedCycle_s = generate_random_within_range(gen);
            }
        }

        m_CardiacCyclePeriod_s = ComputedCycle_s; // Update for next
iteration
        // Print generated RRI for graphing
        std::cout << ComputedCycle_s << std::endl;
    } else {
        // Reset if AF is deactivated

m_data.GetActions().GetPatientActions().RemoveAtrialFibrillation();

```

```

        m_patient->SetEvent(CDM::enumPatientEvent::AtrialFibrillation,
false, m_data.GetSimulationTime());
        m_EnterAtrialFibrillation = false;
        m_StartSystole = true;
        SetHeartRhythm(CDM::enumHeartRhythm::NormalSinus);

GetHeartRate().SetValue(m_data.GetCardiovascular().GetHeartRate().GetVa
lue(), FrequencyUnit::Per_min);
        m_CurrentCardiacCycleDuration_s = 1. /
m_patient->GetHeartRateBaseline().GetValue(FrequencyUnit::Per_s);
        m_CardiacCyclePeriod_s = 0.0;
    }
}

    m_data.GetDataTrack().Probe("m_CardiacCyclePeriod_s ",
m_CardiacCyclePeriod_s);
}

```